Local electron momentum anisotropy in molecules

James L. Anchell and John E. Harriman

Citation: The Journal of Chemical Physics **92**, 2943 (1990); doi: 10.1063/1.458581
View online: http://dx.doi.org/10.1063/1.458581
View Table of Contents: http://scitation.aip.org/content/aip/journal/jcp/92/5?ver=pdfcov
Published by the AIP Publishing

Local electron momentum anisotropy in molecules

James L. Anchell[a] and John E. Harriman
Theoretical Chemistry Institute, University of Wisconsin, Madison, Wisconsin 53706

(Received 20 July 1989; accepted 17 November 1989)

We introduce the Husimi second moment of momentum (SMM) tensor, which is a function of the position of an electron in a molecule. The major axis of the Husimi SMM tensor evaluated at a point **q** gives the most probable line of motion for an electron described by a Gaussian wave packet state centered at that point. We investigate two isoelectronic series: N_2, NO^+, CN^-, CO, and HF, H_2O, NH_3, CH_4. For molecules in the multiply bonded series we discover spatial regions in which electron motion is preferentially parallel or perpendicular to the bond axis. We also find a connection between these two regions and the σ and π symmetry contributions to the density. For molecules in the polyatomic series we observe two characteristic local momentum anisotropies. For electrons near a bond axis the preferred motion tends to be transverse to the bond axis, and for electrons near a plane defined by three atoms the preferred motion is normal to the plane. In all systems, the local anisotropy is typically on the order of 1% of the local isotropic component at the same position.

I. INTRODUCTION

There has been considerable interest in recent years in one-electron momentum distributions in atoms and molecules.[1-13] The work reported here emphasizes the anisotropy of the momentum distribution, particularly the phenomenon known as the bond directionality principle (BDP). While simple ideas suffice to explain this effect in singly bonded diatomics, more sophisticated techniques are required for multiply bonded diatomic, or polyatomic molecules. Sharma and Thakkar[9] have reported global momentum anisotropies obtained as expectation values of components of the kinetic energy, and give a number of references to earlier work on kinetic energy anisotropy. We have found it useful to explore local momentum densities using molecular electronic Husimi functions. We have previously discussed the electronic Husimi function for H and N atoms,[12] and some diatomic molecules.[13] The definition of this function is reviewed in the next section.

For our purposes the BDP may be stated as follows: for a fixed magnitude of the momentum of an electron in a covalently bonded diatomic, it is more probable for the electron to be moving transverse to the bond rather than parallel to it. A more general statement of the BDP may be found elsewhere.[14] The BDP is readily seen in a contour plot of the total momentum density for H_2. See for example Fig. 2(a) of Ref. 13. A mathematical model of the BDP based on either the valence bond or MO description of bonding may be found elsewhere.[15]

Epstein and Tanner[16] provided a simple physical explanation of the BDP: due to buildup of electron density in the internuclear region in the formation of a covalent bond, the charge density, and the total wave function for the system are slowly changing along the bond axis. Conversely, perpendicular to the axis the wave function falls off quickly. Recalling that the momentum-space wave function is the Fourier transform of a the position-space wave function, and that the Fourier transform of a function converts diffuse regions into sharp regions and *vice versa*, one sees the origin of the BDP. This argument does not hold for diatomics that are ionically bonded. Since the bond in an ionic compound arises primarily from the transfer of electron density from one atom to another, one expects the charge density and the total wave function to be approximately the sum of two spherically symmetric components about two centers. The spherical symmetry will be preserved upon Fourier transforming to obtain the wave function in the momentum representation. For example, Fig. 2(b) of Ref. 13 shows no significant BDP in the polar molecule LiH. The absence of a BDP for this species is indicative of an ionically bonded system.

The BDP is also less obvious in the total momentum density for the multiply bonded N_2 molecule (see Fig. 1). It has been shown[13] that in a local description of electron densities, electrons in the bonding region do exhibit a BDP, but this is partially masked in the total momentum density by contribution from electrons in other spatial regions. [See,

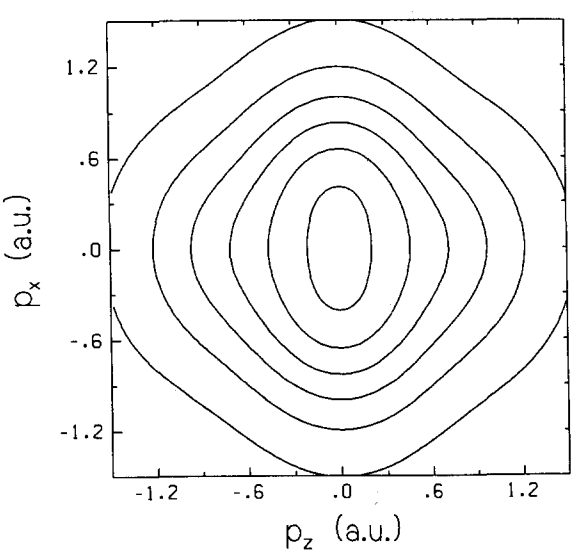

FIG. 1. Total momentum density of N_2. Contours: 0.1 to 1.1 in steps of 0.1.

[a] Present address: Department of Chemistry, University of Utah, Salt Lake City, Utah 84112.

 0021-9606/90/052943-10$03.00

for example, Figs. 14(a) and 14(b) in Ref. 13.] Additional information can be gained by examining separately the contributions from sigma and pi subsystems, or even from individual orbitals.[9,10] Further difficulty arises when one tries to generalize the BDP to nonlinear polyatomics because in these systems there is no satisfactory, single bond direction in which to study the BDP. For example, consider the bent triatomic H_2O. For density studies in position space, one can concentrate on just one of the equivalent O–H bonds at a time, but in momentum space the total density arises from the Fourier transform of all regions in position space, and the two bond axes are not parallel. It will be shown in this paper that one may observe bond directionality in multiply bonded and polyatomic molecules by using a "local momentum anisotropy."

There are advantages to examining momentum anisotropy locally. It is possible to separate different contributions which are difficult to distinguish in a global description, and this can be done without requiring an orbital description or by invoking only the symmetry properties of natural orbitals.

For an S-state atom, the Husimi function depends only on the magnitudes of the coordinate and momentum vectors, and on the angle between them. We found for H and N that the angle dependence is slight, but favors a perpendicular configuration. Another way of examining this effect will be presented below. We have previously reported a number of ways of examining the Husimi function for diatomic molecules, including local momentum density contour plots for sections defined by various, fixed coordinate choices.

Section II of this paper presents relevant formalism associated with the Husimi function and the local momentum anisotropy. Sections III A and III B present results for the multiply bonded systems N_2, CO, CN^-, and NO^+, and for the isoelectronic series HF, H_2O, NH_3 and CH_4. In Sec. IV we summarize our results and suggest possible extensions.

II. FORMALISM

A. The Husimi function

The investigations reported here make use of the Husimi function,[17] which is a quantum phase-space density $\eta(\sigma;\mathbf{q},\mathbf{k})$ giving the probability of finding a particle (in the system being described) in a Gaussian wave packet state with width parameter σ centered in position space at the point $\mathbf{q}$ and in momentum space at the point $\mathbf{k}$. We are concerned with systems of electrons in molecules, in which case the Husimi function can be expressed as

$$\eta(\sigma;\mathbf{q},\mathbf{k}) = \frac{1}{(2\pi)^3}\int\int \phi^*(\sigma;\mathbf{q},\mathbf{k}|\mathbf{r})\gamma(\mathbf{r};\mathbf{r}')\phi(\sigma;\mathbf{q},\mathbf{k}|\mathbf{r}')\,d\mathbf{r}'\,d\mathbf{r}, \tag{1}$$

where $\phi(\sigma;\mathbf{q},\mathbf{k}|\mathbf{r})$ is a three-dimensional Gaussian wave packet (coherent state) with width parameters $\sigma_x = \sigma_y = \sigma_z = \sigma$ and $\gamma(\mathbf{r};\mathbf{r}')$ is the one-electron charge density matrix, i.e., the one-electron reduced density matrix integrated over spin.

We use the Husimi function to allow a phase space probability density to be defined in a way that is consistent with the uncertainty principle. In a Gaussian wave packet state the balance between the uncertainty in momentum and that in position for any (Cartesian) coordinate is determined by the parameter σ. For all of the calculations reported here, σ has been chosen to be 1 in atomic units, to treat different degrees of freedom equivalently. Consequently, the width parameter will be suppressed in the argument of the Husimi function for the remainder of this paper. A more detailed discussion of the relevant properties of the Husimi function can be found elsewhere.[18]

B. Anisotropy of local momentum density

The Husimi function can be used to define a local momentum density by thinking of the position coordinate $\mathbf{q}$ as being fixed and examining the behavior with respect to the remaining momentum coordinates. To avoid conflict with the uncertainty principle, the Husimi function provides a "coarse grained" phase-space description. It can also be obtained by taking a Gaussian convolution of the Wigner function[19] over both position and momentum variables. While integration of the Wigner function over position coordinates gives the total momentum density, similar integration of the Husimi function gives a Gaussian convolution of the total momentum density.

A complete examination of the momentum distribution at each of a representative set of position-space points is not practical for most systems, and since we are concerned here primarily with the anisotropy of the local momentum distribution it is convenient to introduce some measure of that anisotropy. One possibility is provided by the second moments of the Husimi function with respect to the components of the momentum. A "second moment of momentum" (SMM) tensor $\mathsf{T}(\mathbf{q})$ is defined at each point $\mathbf{q}$ with components

$$T_{ab}(\mathbf{q}) = \int \eta(\mathbf{q},\mathbf{k})k_a k_b\,d\mathbf{k}, \quad a,b = x,y,z. \tag{2}$$

This tensor is closely related to one which can be used to describe the local kinetic energy

$$K_{ab}(\mathbf{r}) = \nabla_{r_a}\nabla_{r'_b}\gamma(\mathbf{r};\mathbf{r}')|_{\mathbf{r}'=\mathbf{r}}$$
$$= \int p_a p_b W(\mathbf{q},\mathbf{p})\,d\mathbf{p}, \tag{3}$$

where W is the Wigner function. It is shown in the Appendix that

$$T_{ab}(\mathbf{q}) = \int K_{ab}(\mathbf{r})g(\mathbf{r}-\mathbf{q})\,d\mathbf{r} + \delta_{ab}\sigma^2\int \rho(\mathbf{r})g(\mathbf{r}-\mathbf{q})\,d\mathbf{r}, \tag{4}$$

where g is the normalized Gaussian distribution

$$g(\mathbf{r}-\mathbf{q}) = \left(\frac{\sigma^2}{\pi}\right)^3 e^{-\sigma^2(\mathbf{r}-\mathbf{q})^2}. \tag{5}$$

The first term on the right in Eq. (4) is a Gaussian convolution of K_{ab}, and is to be expected. The second term is a Gaussian convolution of the coordinate density and is thus proportional to the integral of $\eta(\mathbf{q},\mathbf{k})$ over momenta. Note, however, that this term affects only the isotropic part of T and will not contribute to the anisotropy which is our main concern here. If we had chosen different values for the Gaussian widths σ_x, σ_y, and σ_z, this term would not be isotropic

but would still contribute only to the diagonal elements of T. Such an anisotropy would be artificial, introduced by the anisotropy in σ.

The anisotropic part of the SMM tensor is

$$\Delta\mathsf{T}(\mathbf{q}) = \mathsf{T}(\mathbf{q}) - T_{\rm iso}(\mathbf{q})\mathsf{I}, \tag{6}$$

where

$$T_{\rm iso}(\mathbf{q}) = \tfrac{1}{3}\,\mathrm{Tr}\,[\mathsf{T}(\mathbf{q})] \tag{7}$$

and I is the unit tensor. The principal values and the directions of the principal axes of $\Delta\mathsf{T}$ provide a convenient way of describing the anisotropy of local momentum at $\mathbf{q}$. In special cases symmetry allows a further reduction in the number of parameters required. We will use the terms major axis, intermediate axis, and minor axis to refer to the principal axes associated with the largest, middle, and smallest principal values, respectively. *If the momentum of an electron in the vicinity of position* $\mathbf{q}$ *is observed, it will be most likely to be in the direction of the major axis and least likely to be in the direction of the minor axis.* Note, however, that we are dealing with a second moment, so the principal values are all positive and either sign of the momentum along the specified axis is equally likely. For a nondegenerate stationary state, the first moments of the momentum distribution vanish.

For a diatomic molecule we follow the convention of choosing a coordinate system with origin at the center of nuclear charge and z axis along the molecular axis. For points $\mathbf{q}$ on this axis, the local momentum distribution has cylindrical symmetry and T is already diagonal with $T_{xx} = T_{yy}$ for any choice of x and y axes. We can then use the single quantities

$$\begin{aligned} \Delta T(\mathbf{q}) &= 2T_{zz}(\mathbf{q}) - T_{xx}(\mathbf{q}) - T_{yy}(\mathbf{q}), \\ A(\mathbf{q}) &= \Delta T(\mathbf{q})/T_{\rm iso}(\mathbf{q}) \end{aligned} \tag{8}$$

to describe the absolute or relative anisotropy, respectively. If these parameters are zero, then the momentum at $\mathbf{q}$ is isotropic. A negative value indicates a greater probability for observing a momentum perpendicular to the bond than parallel to it, as in the bond directionality principle, while a positive value indicates a greater probability for momentum parallel to the bond.

The absolute and relative anisotropies defined here correspond to a local version of the anisotropy of the kinetic energy and the reduced kinetic energy anisotropy α discussed by Thakkar *et al.*[9,10] In addition to the generalization to a local description, the SMM formulation provides a general tensor that can be used in cases where the principal axis orientations are not completely determined by symmetry.

When there is symmetry, it can be used to simplify the description. Suppose that $\mathscr{M}$ is a symmetry plane for the system of interest, and that the field point $\mathbf{q}$ at which T is to be evaluated lies in $\mathscr{M}$. For an atom or diatomic molecule any field point is possible, with $\mathscr{M}$ chosen to contain $\mathbf{q}$ and the nucleus or nuclei. For polyatomic molecules having a symmetry plane, a restricted set of $\mathbf{q}$'s can be chosen lying in $\mathscr{M}$. In any of these cases it can be shown that one principal axis of T will be perpendicular to $\mathscr{M}$ while the others lie in $\mathscr{M}$.

We want to reserve z for the molecular axis, so we choose a coordinate system with $\mathscr{M}$ in the zx plane. The SMM tensor will then be of the form

$$\mathsf{T}(\mathbf{q}) = \begin{pmatrix} T_{xx}(\mathbf{q}) & 0 & T_{xz}(\mathbf{q}) \\ 0 & T_{yy}(\mathbf{q}) & 0 \\ T_{zx}(\mathbf{q}) & 0 & T_{zz}(\mathbf{q}) \end{pmatrix}. \tag{9}$$

The y axis is a principal axis and the block form of the tensor is more apparent if the axes are cyclically reordered as zxy instead of as xyz. The zx block can be written as

$$\begin{aligned} \begin{pmatrix} T_{zz}(\mathbf{q}) & T_{zx}(\mathbf{q}) \\ T_{xz}(\mathbf{q}) & T_{xx}(\mathbf{q}) \end{pmatrix} &= t_0(\mathbf{q})\mathbf{1} + \mathbf{t}(\mathbf{q}) \\ &= \begin{pmatrix} \mathrm{t}_0(\mathbf{q}) & 0 \\ 0 & t_0(\mathbf{q}) \end{pmatrix} + \begin{pmatrix} a(\mathbf{q}) & b(\mathbf{q}) \\ b(\mathbf{q}) & -a(\mathbf{q}) \end{pmatrix}, \end{aligned} \tag{10}$$

where

$$\begin{aligned} t_0(\mathbf{q}) &= \tfrac{1}{2}[T_{zz}(\mathbf{q}) + T_{xx}(\mathbf{q})], \\ a(\mathbf{q}) &= \tfrac{1}{2}[T_{zz}(\mathbf{q}) - T_{xx}(\mathbf{q})], \\ b(\mathbf{q}) &= T_{zx}(\mathbf{q}) = T_{xz}(\mathbf{q}). \end{aligned} \tag{11}$$

The remaining principal values are $t_0(\mathbf{q}) \pm |\lambda(\mathbf{q})|$, where $\lambda^2(\mathbf{q}) = a^2(\mathbf{q}) + b^2(\mathbf{q})$. We will identify the three principal values of $\Delta\mathsf{T}$ in this case as

$$\begin{aligned} \Delta T_1(\mathbf{q}) &= t_0(\mathbf{q}) + |\lambda(\mathbf{q})| - T_{\rm iso}(\mathbf{q}), \\ \Delta T_2(\mathbf{q}) &= t_0(\mathbf{q}) - |\lambda(\mathbf{q})| - T_{\rm iso}(\mathbf{q}), \\ \Delta T_3(\mathbf{q}) &= T_{yy}(\mathbf{q}) - T_{\rm iso}(\mathbf{q}). \end{aligned} \tag{12}$$

Note that $\Delta T_1(\mathbf{q}) \geqslant \Delta T_2(\mathbf{q})$. These quantities, together with the orientations of the principal axes, provide a characterization of the local momentum anisotropy.

Suppose that a plane $\mathscr{M}$ and coordinate system have been chosen and we want to examine $\mathsf{T}(\mathbf{q})$ for various field points in $\mathscr{M}$. A convenient way to summarize the results diagramatically is as follows: A figure is constructed for the zx plane $\mathscr{M}$. At each of a representative set of points in the plane, a double-headed arrow is drawn with its length proportional to ΔT_1 and its direction that of the corresponding principal axis. If an observation could be made of the in-plane component of the momentum of an electron in the vicinity of $\mathbf{q}$, it would be most likely to be in the indicated direction and least likely to be perpendicular to that direction, while the length of the arrow provides an indication of the difference between these probabilities.

Note that although $\Delta T_1 \geqslant \Delta T_2$, by definition, the relationship of ΔT_3 to ΔT_1 or ΔT_2 is not determined by general considerations: the y axis may be the major, intermediate, or minor principal axis. In cases of high symmetry, such as $\mathbf{q}$ on the axis of a diatomic molecule or any point in an atom, $\Delta T_3 = \Delta T_1$ or $\Delta T_3 = \Delta T_2$. In such cases a single value determines all three ΔT_j, since their sum is always zero. Some information about ΔT_3 can be provided in the figure by using a filled circle at $\mathbf{q}$ to indicate that $\Delta T_3(\mathbf{q}) \geqslant \Delta T_1(\mathbf{q})$.

While an $\mathscr{M}$-plane figure of the type discussed above gives a compact representation of the global behavior of $\Delta\mathsf{T}$, it does not provide complete information about the $\Delta T_j(\mathbf{q})$ or any information about $T_{\rm iso}(\mathbf{q})$. An alternative approach is to define a line in the molecular coordinate space and to plot $T_{\rm iso}(\mathbf{q})$ and the $\Delta T_j(\mathbf{q})$ as functions of position along

this line. If the principal axis directions are not determined by symmetry, they can also be indicated. We will use both of these methods of summarizing data in what follows.

III. RESULTS

A. Electronic calculations

All data presented here on the isoelectronic diatomic systems N_2, CO, CN^-, and NO^+ were derived from the one-electron spinless density matrix obtained from a configuration interaction calculation with single and double excitations using a standard Pople 6-311G basis set[20] and the *ab initio* program GAMESS.[21] We compared SCF and CI results and performed an auxiliary calculation on N_2 with a Dunning (5*s*,4*p*) basis set,[22,23] which uses two *s*-type basis functions to describe the core. Quantitatively, the results were only slightly changed, and qualitatively we found nothing different in our results. We did not include *d* functions, which significantly increase the complexity of our analysis, especially when sigma and pi contributions are to be separated. We expect that there would be no qualitative changes and only minor quantitative changes if such functions were included. For HF, H_2O, NH_3, and CH_4 the calculations were performed at the restricted Hartree–Fock level using a standard Pople 6-31G* basis.[24] For this purpose we used the *ab initio* program GAUSSIAN 86.[25]

The bond lengths of the multiply bonded diatomics were obtained from experimental data,[26] and the bond lengths and bond angles of the series isoelectronic to HF were obtained by geometry optimization. The distances are given in Table I.

We also present some results on the hydrogen atom which serves as a preliminary to our discussion. This calculation was performed using an even tempered basis set[27] with 20 *s*-type functions, and was carried out with the GAMESS package.

B. Hydrogen and nitrogen atoms

Figure 2 schematically presents the results of our calculation of the Husimi SMM tensor for the hydrogen atom. In the atomic case, every point is of special symmetry so that $\Delta T_1(\mathbf{q}) = \Delta T_3(\mathbf{q})$. At each field point studied it was found that $\Delta T_1(\mathbf{q})$ and $\Delta T_3(\mathbf{q})$ were greater than zero, and $\Delta T_2(\mathbf{q})$ was less than zero. The directions of the principal moments in the plane $\mathcal{M}$ show that measurements of the electron momentum would find the most probable direction of motion to be at a right angle to the radius vector from the nucleus to the field point. This is consistent with results obtained previously.[12] Additionally, it is worthy of note that

TABLE I. Bond lengths and angles used in calculations.[a]

	N_2	NO^+	CN^-	CO	HF	H_2O	NH_3	CH_4
r (a.u.)	2.075	1.966	2.192	2.132	1.721	1.823	1.899	2.048
∠HXH	...	...	...	...	...	105.5	107.2	109.5

[a] For diatomics *r* is the bond length, and for the polyatomics *r* is the distance from the central atom to a hydrogen. ∠HXH is the angle between two XH bonds.

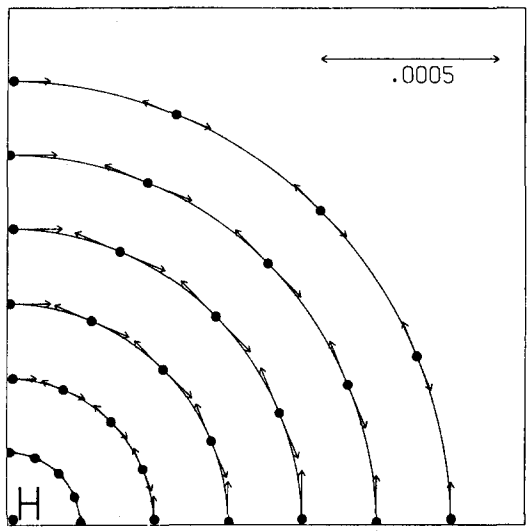

FIG. 2. Representation of the Husimi SMM tensor for hydrogen atom. The nucleus is at the origin. The concentric quarter circles have radii equal to 0.25 to 1.5 in increments of 0.25. The field points which lie on these circles were evaluated at angles of 0 to 90 deg in increments of 22.5.

$\Delta T_1(\mathbf{q})$ is greatest at a radius of 1 a.u., indicating that this probability is the greatest at the first Bohr radius.

We have also examined the SMM tensor for the nitrogen atom—not only for the total electronic Husimi function, but also for contributions from *s* and *p* orbitals. In each case the result is qualitatively similar to that obtained for the hydrogen atom: $\Delta T_1(\mathbf{q}) = \Delta T_3(\mathbf{q})$ and $\Delta T_2(\mathbf{q}) \leqslant 0$. We observed that the magnitude of the *s* orbital contribution to the anisotropy was slightly greater than the *p* orbital contribution, and that this relative difference increased as the distance of the field point from the nucleus decreased.

C. Multiply bonded diatomics

Figure 3 shows results obtained from the evaluation of the Husimi SMM tensor for CO. We again use a coordinate system with origin at the center of nuclear charge and *z* axis along the internuclear axis. Very similar results were obtained for N_2, NO^+, and CN^-. The one notable difference among the members of this isoelectronic series is that for the heteronuclear diatomics the principal axes associated with $\Delta T_1(\mathbf{q})$ for $\mathbf{q}$ at a 90 deg angle from the bond axis were tilted

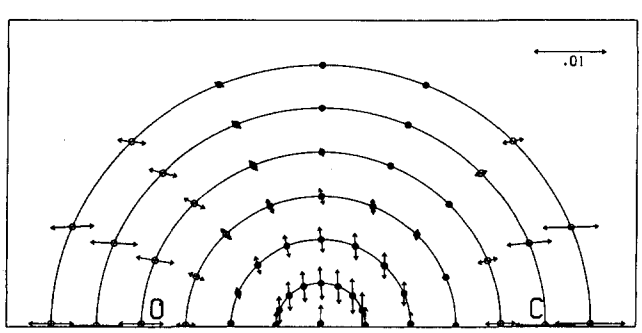

FIG. 3. Representation of the Husimi SMM tensor for CO. The origin is at the center of nuclear charge. Field points are shown with radii 0.25 to 1.5 in increments of 0.25 and angles from 0 to 180 deg in increments of 22.5 deg.

slightly toward the lighter atom. By comparison, for any homonuclear species such as N_2 symmetry dictates that a similar calculation must show that the principal axes are directed either parallel or perpendicular to a ray passing from the origin to such a field point. Most of the following discussion is applicable to any member of the isoelectronic series.

There are two regions in the $\mathcal{M}$ plane for which the values of $\Delta T_1(\mathbf{q})$ are relatively large. Near the origin, region I, the axes corresponding to $\Delta T_1(\mathbf{q})$ are nearly perpendicular to the bond axis. At field points at a distance from the origin comparable to or somewhat greater than that of a nucleus, and at an angle less than about 45 deg (or greater than about 135 deg), region II, $\Delta T_1(\mathbf{q})$ again is relatively large in magnitude, but now the associated axis is directed nearly parallel to the bond axis. At other field points we observe that $\Delta T_1(\mathbf{q})$ is quite small by comparison.

The total momentum density of N_2 (Fig. 1) shows that for low momenta there is a preference for the electron's momentum to be oriented perpendicular to the bond, but for momenta greater that about 0.5 a.u. there is increased probability of orientation either transverse or parallel to the bond, with reduced probability of orientations at intermediate angles. Recall that one expects to find electrons with high momentum near to either nucleus (where the nuclear Coulomb potential is of large magnitude), and the low momentum electrons are expected to be located far from the nuclei.

Compared to region II, region I is relatively far from the nuclei, so electrons in this region should carry relatively lower momenta. From Fig. 3 we see that the increased probability of finding electrons with low momenta moving transverse to the bond axis, shown in the total momentum density of Fig. 1, is contributed mainly from electrons in region I, and the increased probability of finding electrons with momenta greater than about 0.5 whose motion is parallel to the bond axis is contributed mainly from electrons in region II.

Further insight may be gained by decomposing the Husimi SMM density into components contributed by the σ and π symmetry components of the charge density matrix. Although $T_{\text{iso}}(\mathbf{q})$ was found to be strongly dominated by the σ contribution, σ and π contributions to $\Delta T(\mathbf{q})$ were of comparable magnitude. Figure 4 shows the $\Delta T_j(\mathbf{q})$ results obtained for the σ and π components of the Husimi SMM density for N_2. The differences are striking. At all field points the major axis in the σ picture is aligned with the bond axis to within 1 deg. The π picture shows the major axis strongly aligned transverse to the bond axis. Additionally, we found that the major and minor axes in the σ picture are always in the $\mathcal{M}$ plane, and the intermediate axis is directed out of the plane. On the other hand, the π picture shows that the major axis is always directed out of the plane. This latter observation corresponds well to our intuition that the π electrons possess nonzero L_z angular momentum. Additionally, we see that although some cancellation between the σ and π contributions to the total Husimi SMM density will occur, it is the σ contribution which is responsible for the buildup of density directed parallel to the bond axis, and it is the π contribution which gives rise to the buildup of density directed transverse to the bond. Hence in the total momentum density the increased probability of finding electrons moving parallel to the bond axis in some coordinate regions is attributable to the σ electron density, while in other coordinate regions increased probability of finding electrons moving transverse to the bond axis is attributable to the π electron density. We substantiate this finding by carrying out a σ–π decomposition of the total momentum density, which is shown in Figs. 5 and 6. We observe that the σ density is elongated along the bond axis, and that the π density is elongated transverse to the axis—this being consistent with Husimi SMM analysis.

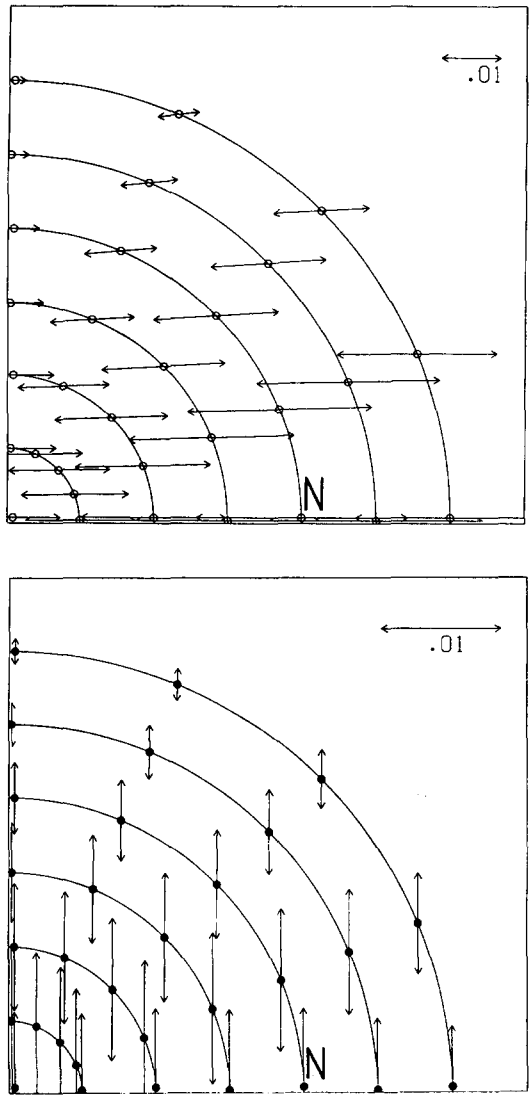

FIG. 4. (a) σ and (b) π contribution to the Husimi SMM tensor for N_2. The locations of the field points are the same as those in the right half of Fig. 3.

These results are completely consistent with the results of Thakkar *et al.*[10] who showed that for B_2, C_2, N_2, O_2, and F_2 the bond-parallel component of the expectation value of the kinetic energy $T_{\|}$ is greater than the transverse component $T_{\perp}$ for sigma orbitals while $T_{\|} < T_{\perp}$ for pi orbitals.

The field points represented by filled circles in Fig. 3 show that $\Delta T_3(\mathbf{q})$ is more likely to correspond to the major axis for small values of the radius and angles approaching 90

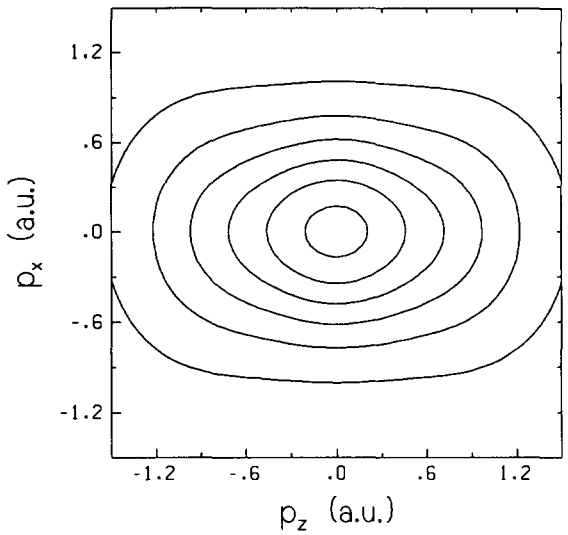

FIG. 5. σ component of the total momentum density of N_2. Contours: 0.2 to 1.2 in steps of 0.2.

deg. A more quantitative description of the relationship between $\Delta T_1(\mathbf{q})$, $\Delta T_2(\mathbf{q})$, and $\Delta T_3(\mathbf{q})$ may be gained from study of Table II, which gives values of $\Delta T_1(\mathbf{q})$, $\Delta T_2(\mathbf{q})$, $\Delta T_3(\mathbf{q})$, and $T_{\rm iso}(\mathbf{q})$ for various field points for N_2.

The first thing to notice is that $T_{\rm iso}(\mathbf{q})$ is two orders of magnitude larger than $\Delta T_1(\mathbf{q})$, $\Delta T_2(\mathbf{q})$, or $\Delta T_3(\mathbf{q})$. This indicates that as a first approximation the SMM density is isotropic, and measurements of electron momenta would show essentially random orientations. However, the fact that the $\Delta T_j(\mathbf{q})$ are not all zero indicates that if enough measurements were made one would be able to detect a slight preference in the orientation at $\mathbf{q}$. Additionally, it can be seen from the previous figures that definite spatial patterns emerge with respect to the principal values and axes of ΔT. One should also note that $\Delta T_2(\mathbf{q})$ is less than zero at all angles studied. By definition $\Delta T_2(\mathbf{q}) \leqslant \Delta T_1(\mathbf{q})$, but we also observe that $\Delta T_2(\mathbf{q}) \leqslant \Delta T_3(\mathbf{q})$ everywhere.

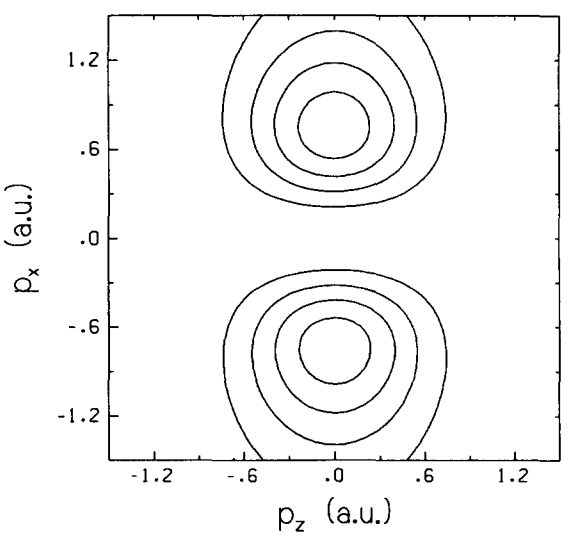

FIG. 6. π component of the total momentum density of N_2. Contours: 0.1 to 0.4 in steps of 0.1.

TABLE II. SMM tensor for N_2.

R	$T_{\rm iso}$	100× $\Delta T_1(\mathbf{q})$	100× $\Delta T_2(\mathbf{q})$	100× $\Delta T_3(\mathbf{q})$
		0 deg		
0.00	1.157	0.481	−0.961	0.481
0.25	1.137	0.385	−0.770	0.385
0.50	1.300	0.136	−0.271	0.136
0.75	1.466	0.346	−0.173	−0.173
1.00	1.538	0.860	−0.430	−0.430
1.25	1.458	1.115	−0.557	−0.557
1.50	1.233	1.082	−0.541	−0.541
		45 deg		
0.00	1.157	0.481	−0.961	0.481
0.25	1.072	0.414	−0.851	0.437
0.50	1.062	0.243	−0.559	0.317
0.75	1.008	0.134	−0.314	0.180
1.00	0.890	0.292	−0.365	0.073
1.25	0.716	0.441	−0.459	0.018
1.50	0.519	0.468	−0.476	0.008
		90 deg		
0.00	1.157	0.481	−0.961	0.481
0.25	1.009	0.436	−0.917	0.482
0.50	0.843	0.322	−0.801	0.480
0.75	0.625	0.185	−0.646	0.460
1.00	0.421	0.069	−0.485	0.416
1.25	0.241	−0.006	−0.343	0.350
1.50	0.127	−0.043	−0.231	0.273

We see from Fig. 3 that when the Husimi SMM tensor is evaluated on the bond axis, the principal axis which is at 90 deg to the bond axis switches from being the major axis to being the minor axis at a field point roughly midway from the origin to either nucleus. By symmetry, the principal value associated with the axis normal to the $\mathscr{M}$ plane must be equal to that associated with the principal axis directed at 90 deg to the bond axis, when the Husimi SMM tensor is evaluated on a field point which lies on the bond axis. These two observations are supported by the $\Delta T_3(\mathbf{q})$ values in Table II.

Along the bond axis (0°) $\Delta T_3(\mathbf{q}) = \Delta T_1(\mathbf{q})$ for $R \leqslant 0.50$ while $\Delta T_3(\mathbf{q}) = \Delta T_2(\mathbf{q})$ for $R \geqslant 0.75$. There appears to be a special point near $R = 0.6$ where all three values are equal, and thus necessarily zero. When the 0° values are plotted as a function of R there is what looks like an avoided crossing between the $\Delta T_1(\mathbf{q})$ and $\Delta T_2(\mathbf{q})$ curves at this point. At this special point on the axis, the SMM tensor is completely isotropic.

For 0° $\Delta T_3(\mathbf{q}) \leqslant \Delta T_1(\mathbf{q})$ for all R, while for 180° $\Delta T_3(\mathbf{q}) \geqslant \Delta T_1(\mathbf{q})$ for all R. When the angle is 45°, $\Delta T_3(\mathbf{q}) \geqslant \Delta T_1(\mathbf{q})$ for R up to about 0.8 but $\Delta T_3(\mathbf{q}) \leqslant \Delta T_1(\mathbf{q})$ for larger R.

It is also apparent that all of the anisotropies approach zero asymptotically. This is predictable since the Husimi function itself will go asymptotically to zero in any direction.

D. First row hydrides AH_n

Figures 7 through 10 show the results obtained from the evaluation of the Husimi SMM tensor for HF, H_2O, NH_3, and CH_4. In all cases the $\mathscr{M}$ plane was chosen so that one principal axis of ΔT was required by symmetry to be normal to it. For HF this plane is defined by the same convention

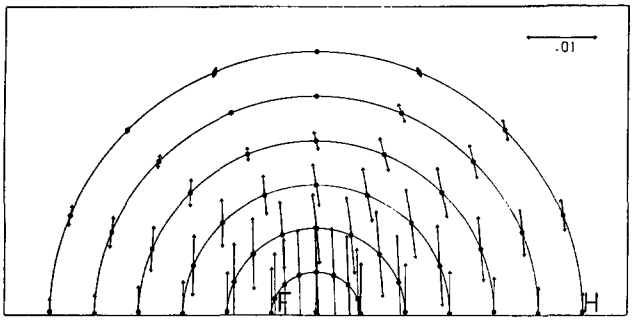

FIG. 7. Representation of the Husimi SMM tensor for HF. The origin is at the center of nuclear charge. The radii of the half circles range from 0.5 to 2.5 in increments of 0.5. The angles that the radius vectors make to the bond axis are the same as in Fig. 3.

used for the multiply bonded diatomics of the preceding section. For H_2O, NH_3, and CH_4 the $\mathscr{M}$ plane is more constrained. For these molecules the heavy atom is situated at the origin and the z axis is collinear with a principal symmetry axis. For NH_3 one of the hydrogens lies in the zx plane, $\mathscr{M}$, and the other two hydrogens are situated symmetrically above and below the plane. For H_2O and CH_4 two hydrogens lie in the zx plane, and the remaining two hydrogens of CH_4 are situated symmetrically above and below the plane. The chemical symbols in each of the figures represent the locations of the atoms in the molecule and the $\times$'s indicate the positions of the projections of the out of the plane hydrogens.

1. HF

The Husimi SMM tensors for HF plotted in Fig. 7 show that the most probable orientation of the in-plane component of the electron momentum is transverse to the bond axis everywhere, unlike the multiply bonded diatomics. The darkened field points indicate that the most probable orientation of the momentum of the electron is normal to the $\mathscr{M}$ plane. Along the bond axis $\Delta T_1(\mathbf{q}) = \Delta T_3(\mathbf{q})$ by symmetry, and at 90 deg to the bond axis both $\Delta T_1(\mathbf{q})$ and $\Delta T_3(\mathbf{q})$ decrease monotonically as the displacement from the molecule increases.

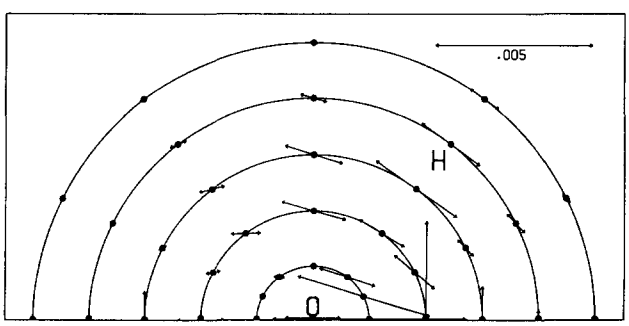

FIG. 8. Representation of the Husimi SMM tensor for H_2O. The oxygen atom is at the origin. The field points lie along lines which are: coincident with the C_2 axis; at angles halfway between the C_2 axis and the bond axes; coincident with the bond axes; and at a 90 deg angle to the C_2 axis. The radii of the circles are the same as those in Fig. 3.

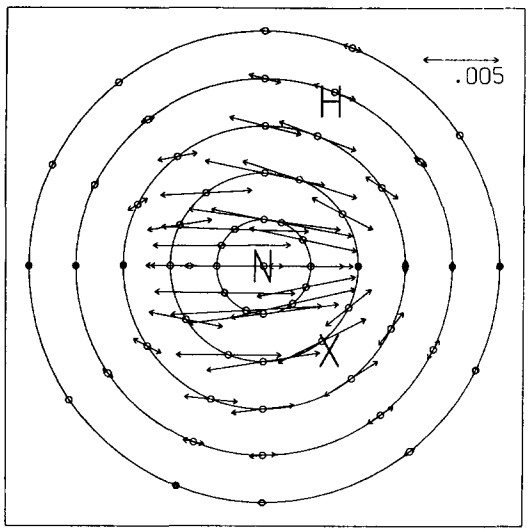

FIG. 9. Representation of the Husimi SMM tensor for NH_3. The nitrogen atom is at the origin. The field points lie along lines which are: coincident with the C_3 axis; at an angle halfway between the C_3 axis and the bond axis; coincident with the bond axis; at a 90 deg angle to the C_3 axis; at angle half the distance from the C_3 axis and the line $\mathscr{L}$ passing through the origin and the projection of the out of plane hydrogens, $\times$; and coincident with the line $\mathscr{L}$. The radii of the circles are the same as those in Fig. 3.

Sharma and Thakkar[9] found a negative kinetic energy anisotropy (a transverse orientation in our terminology) for HF and showed that it arises from a nonbonding orbital of pi symmetry on F. While we did not separate sigma and pi contributions for this molecule, a comparison of our results with those of Sharma and Thakkar suggests that the momentum distribution throughout the molecule is dominated by the F contribution. This is consistent with what is known about the total coordinate density of HF.

2. H_2O

We observe a BDP in Fig. 8. That is, for most field points on the bond axis $\Delta T_1(\mathbf{q})$ is aligned transverse to the

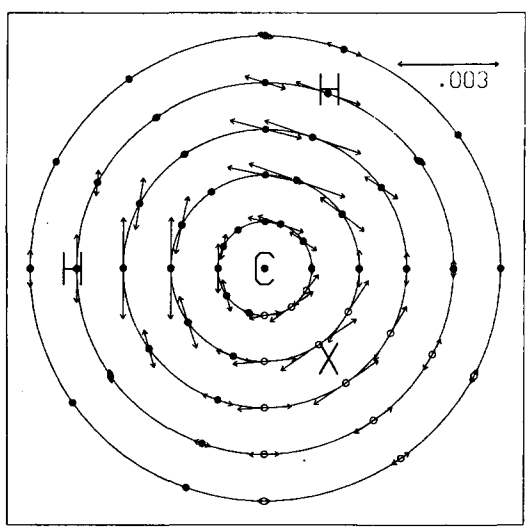

FIG. 10. Representation of the Husimi SMM tensor for CH_4. The carbon atom is at the origin. The field points may be described as in Fig. 9.

bond, and this alignment becomes more pronounced as the displacement from oxygen increases. One way of understanding this result is to consider a model for H_2O in which the bond of interest is represented by an OH^- perturbed by an H^+. We expect OH^- to have a Husimi SMM density similar to that for HF. The perturbing H^+ will affect those electrons closer to it—in this case those closer to the oxygen.

The physical explanation[16] of the bond directionality principle for diatomics pointed out that where the wave function—and hence density—was quickly varying one expected the momentum density to be elongated. This stretching of the momentum density represents an increased probability of finding an electron moving in the direction of the elongation. For H_2O the density varies quickly in the direction perpendicular to the plane of the molecule, and varies more slowly within the plane. Therefore it is not surprising that we find $\Delta T_3(\mathbf{q}) \geqslant \Delta T_1(\mathbf{q})$, for all values of $\mathbf{q}$ studied—i.e, that the most probable direction of the electrons motion is normal to the plane of the molecule. This propensity for the electron to move transverse to a plane containing a set of atoms will be shown again when we study CH_4.

Figure 11 shows the behavior of $T_{iso}(\mathbf{q})$, $\Delta T_1(\mathbf{q})$, $\Delta T_2(\mathbf{q})$, and $\Delta T_3(\mathbf{q})$ evaluated at points $\mathbf{q}$ which lie along the line of one of the OH bonds. As with HF we see that $\Delta T_3(\mathbf{q})$ decreases monotonically as the displacement from the central region of the molecule increases. However $\Delta T_1(\mathbf{q})$, which is connected to the increased probability for the electron to move at right angles to the bond, does not demonstrate such simple behavior. In fact near the oxygen atom, where we expect the perturbation from the second H atom to be quite large, we see that $\Delta T_1(\mathbf{q})$ actually becomes negative. It is in this region where we find that $\Delta T_3(\mathbf{q})$ is greatest.

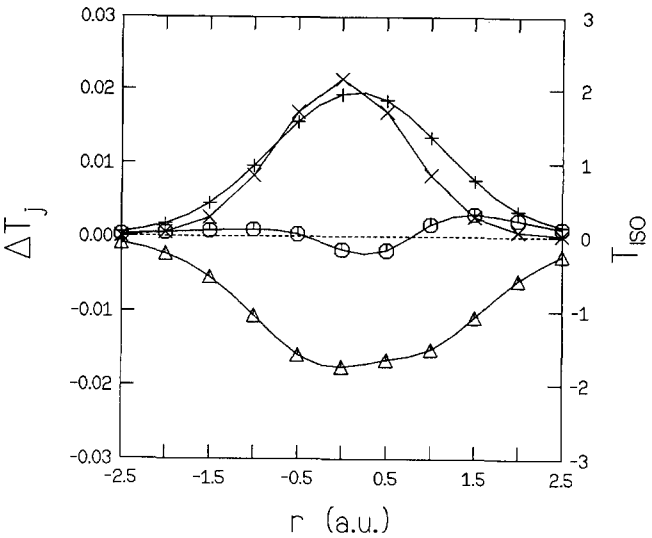

FIG. 11. Values of $\Delta T_j(\mathbf{q})$ and $T_{iso}(\mathbf{q})$ evaluated along an OH bond direction in H_2O. The O atom is at $R = 0$ and the H atom is at $R = +1.8$ a.u. Hexagons indicate values of $\Delta T_1(\mathbf{q})$, triangles values of $\Delta T_2(\mathbf{q})$, $+$'s values of $\Delta T_3(\mathbf{q})$, and $\times$'s values of $T_{iso}(\mathbf{q})$.

3. NH_3 and CH_4

Figures 9 and 10 show representations of the Husimi SMM tensors for NH_3 and CH_4. In each the electrons situated between the heavy atom and one of the hydrogens demonstrate a BDP—that is the principal moment associated with $\Delta T_1(\mathbf{q})$ is oriented transverse to the bond. Due to the high symmetry of CH_4 the orientation of the principal moment in the plane must be exactly 90 deg to the bond (or C_3) axis. It is this property which gives Fig. 10 the appearance of arrows circulating around the molecule with near spherical symmetry. On the other hand, the lack of tetrahedral symmetry in NH_3 allows the principal axis in the bonding region to deviate from 90 deg to the bond axis. As in H_2O, this deviation decreases at field points located further from the central atom. Additionally, in NH_3 we do not see the circular pattern of arrows observed in CH_4. Near the central atom the preferred motion of the electron is parallel to the C_3 axis. At field points far from N and not near a bond axis we observe zones of near isotropy.

In CH_4 we see that $\Delta T_3(\mathbf{q}) \geqslant \Delta T_1(\mathbf{q})$ for about 3/4 of the field points studied. The explanation for this phenomenon is similar to the one given for the behavior of $\Delta T_3(\mathbf{q})$ in H_2O. We may partition the plane $\mathscr{M}$ into two subsets, which we will refer to as $\mathscr{M}_1$ and $\mathscr{M}_2$. $\mathscr{M}_1$ will be that region of the plane $\mathscr{M}$ for which $\Delta T_3(\mathbf{q}) \geqslant \Delta T_1(\mathbf{q})$. Note that in Fig. 10 the two hydrogens which lie in the $\mathscr{M}$ plane also lie in $\mathscr{M}_1$. As in H_2O we expect the position density to be slowly varying in the $\mathscr{M}_1$ plane and quickly varying normal to $\mathscr{M}_1$, so that $\Delta T_3(\mathbf{q}) \geqslant \Delta T_1(\mathbf{q})$. By symmetry the Husimi SMM tensor must be the same when evaluated in the plane $\mathscr{N}$, containing the C atom and two hydrogen atoms whose projections in the $\mathscr{M}$ plane are indicated with an $\times$. We may partition the plane $\mathscr{N}$ into two parts $\mathscr{N}_1$ and $\mathscr{N}_2$ exactly as was done for the plane $\mathscr{M}$. We note that the intersection of $\mathscr{N}_1$ with $\mathscr{M}$ is a ray $\mathscr{R}$ which lies in $\mathscr{M}_2$, and begins at the origin and passes through the projection, $\times$. By the equivalence of $\mathscr{M}$ to $\mathscr{N}$ one sees that for field points evaluated along this ray $\Delta T_1(\mathbf{q})$ must be greater than $\Delta T_3(\mathbf{q})$, and that the orientation of the principal moment corresponding to $\Delta T_1(\mathbf{q})$ must be perpendicular to $\mathscr{R}$. Since the functions involved vary continuously it is reasonable that in the region near $\mathscr{R}$ (i.e., $\mathscr{M}_2$), that $\Delta T_1(\mathbf{q}) \geqslant \Delta T_3(\mathbf{q})$.

For NH_3, the symmetry plane we chose to study contained only two atoms. Therefore one does not see in the figure provided this sort of "polyatomic" BDP, and we expect that in a plane containing two H atoms and the N atom that the most probable momentum for the electron would be such that it is directed nearly normal to that plane. We further expect that the deviation of this orientation from 90 deg to the plane should decrease as the distance of the field point from the perturbing out-of-plane hydrogen increases.

IV. SUMMARY AND DISCUSSION

We have introduced the Husimi second moment of the momentum (SMM) tensor, which may be used as a measure of the anisotropy of the momentum subspace of the quantum phase space described by the Husimi function. The Husimi function description allows us to consider coordinates and momenta simultaneously to the maximum extent allowed by the uncertainty principle. The principal moment of the SMM tensor evaluated at a point $\mathbf{q}$ in coordinate space is

oriented to give the most probable line of motion of a particle observed in the vicinity of that point. For the molecular systems studied we found the motion of electrons to be nearly isotropic. However, we did find identifiable patterns of anisotropic behavior.

For the atomic systems H and N, SMM analysis is consistent with earlier work[12] showing that an electron is most likely to be moving in a direction perpendicular to the radius vector drawn from the nucleus to the electron position.

For N_2, CO, CN^-, and NO^+ we found that in the bond region the principal moment of the Husimi SMM tensor is perpendicular to the bond, as expected from a simple bond directionality viewpoint. However, near the molecular axis but further from the central region we found that the principal moments aligned more nearly parallel to the bond. Decomposing of Husimi SMM tensor into its contributions from σ and π natural orbitals, we found that the principal moments for the π component were perpendicular to the plane containing the bond axis, and the largest components in the plane of the figure were found to be directed perpendicular to the bond axis. The principal moments for the σ component were strongly aligned parallel to the bond axis.

The results obtained here as well as earlier results make it clear that the total momentum density and global kinetic energy anisotropies arise as a sum of contributions, some of which tend to cancel. Even in the simplest case of H_2, electrons with different orientations of their momenta show different redistributions as the chemical bond is formed.[13] This homonuclear molecule with a single sigma bond shows a definite BDP. The ionic molecule LiH, on the other hand, does not. In HF a naive picture again suggests a single sigma bond and the preferred momentum orientation is transverse to the bond everywhere in the molecule. Expectation values of the kinetic energy components[9] show, however, that the 3σ bonding orbital makes a net longitudinal contribution and that a transverse contribution from the 1π nonbonding orbital is responsible for the overall behavior. We do not find a spatial resolution of longitudinal and transverse orientations for this molecule, but have not separated σ and π contributions. For N_2 and isoelectronic species we do find such a spatial resolution, as noted above. In the orbital breakdown of global kinetic energy anisotropies for N_2,[10] the $3\sigma_g$ contribution is longitudinal while the $1\pi_u$ contribution is transverse. We find these orientations to be consistent throughout space for the σ and π contributions to the Husimi SMM tensor, but it is apparent that different contributions are dominant in different spatial regions in the total SMM tensor.

Investigation of H_2O, NH_3, and CH_4 showed a local bond directionality principal: electrons in the vicinity of a bond axis were found to have an increased probability of having their momentum directed transverse to it, and wherever a plane of three adjacent atoms was defined, the most probable direction of the electron motion was normal to this plane. This last observation may be viewed as a generalization of the BDP to polyatomic molecules. In the spatial regions where one expects "lone pairs" to be concentrated, the momentum distribution appears to be quite isotropic.

The anisotropic part of the Husimi SMM tensor is a Gaussian convolution of the anisotropic part of a local kinetic energy tensor, the trace of which is just the kinetic energy of the system. Previous global kinetic energy anisotropies[9,10] are consistent with our local SMM results. The isotropic part of the Husimi SMM tensor includes a contribution proportional to a Gaussian convolution of the coordinate density. The significance of this contribution remains to be clarified.

The work presented here gives some insight into the local momentum behavior of electrons in a number of molecules and allows concepts previously developed for diatomic molecules to be applied to polyatomics as well. It will be of interest to apply these techniques to systems with other kinds of bonding, such as aromatics, hydrogen-bonded, and van der Waals systems, and to changes accompanying chemical reactions or changes in geometry or electronic state would also be of interest.

ACKNOWLEDGMENT

The work reported in this paper was supported by the National Science Foundation through Grant No. CHE-8519723.

APPENDIX: ANALYTIC FORM OF THE HUSIMI SMM TENSOR

We develop here the analytic expression for the elements of $\mathsf{T}(\mathbf{q})$ which appears in Eq. (4). We begin with the definition of the Husimi function given in Eq. (1) generalized to allow for different wave packet widths in different directions:

$$\eta(\boldsymbol{\sigma};\mathbf{q},\mathbf{k}) = \frac{1}{(2\pi)^3}\int\int \phi^*(\boldsymbol{\sigma};\mathbf{q},\mathbf{k}|\mathbf{r})\gamma(\mathbf{r};\mathbf{r}') \times\phi(\boldsymbol{\sigma};\mathbf{q},\mathbf{k}|\mathbf{r}')d\mathbf{r}'\,d\mathbf{r}, \tag{A1}$$

where $\phi(\boldsymbol{\sigma};\mathbf{q},\mathbf{k}|\mathbf{r})$ is a Gaussian wave packet in the $\mathbf{r}$ representation centered at $\mathbf{q}$ and $\mathbf{k}$ with width vector $\boldsymbol{\sigma} = (\sigma_x,\sigma_y,\sigma_z)$. It is given by

$$\phi(\boldsymbol{\sigma};\mathbf{q},\mathbf{k}|\mathbf{r}) = \frac{(\sigma_x\sigma_y\sigma_z)^{1/2}}{\pi^{3/4}} \times\exp\left\{-\frac{1}{2}[\boldsymbol{\sigma}\cdot(\mathbf{r}-\mathbf{q})]^2 + i\mathbf{k}\cdot\mathbf{r}\right\}. \tag{A2}$$

We make the change of variables

$$\Delta\mathbf{r} = \mathbf{r}-\mathbf{r}', \quad \bar{\mathbf{r}} = (\mathbf{r}+\mathbf{r}')/2, \tag{A3}$$

and note that

$$d\mathbf{r}\,d\mathbf{r}' = d(\Delta\mathbf{r})\,d\bar{\mathbf{r}}. \tag{A4}$$

Substitution of Eqs. (A2), (A3), and (A4) into Eq. (A1) gives

$$\eta(\boldsymbol{\sigma};\mathbf{q},\mathbf{k}) = \frac{1}{(2\pi)^3}\int\int \Upsilon(\bar{\mathbf{r}},\Delta\mathbf{r})f(\boldsymbol{\sigma};\mathbf{q}|\bar{\mathbf{r}},\Delta\mathbf{r}) \times\exp(i\,\mathbf{k}\cdot\Delta\mathbf{r})d(\Delta\mathbf{r})\,d\bar{\mathbf{r}}, \tag{A5}$$

where $\Upsilon(\bar{\mathbf{r}},\Delta\mathbf{r}) = \gamma(\bar{\mathbf{r}}+\Delta\mathbf{r}/2;\bar{\mathbf{r}}-\Delta\mathbf{r}/2)$, and

$$f(\boldsymbol{\sigma};\mathbf{q}|\bar{\mathbf{r}},\Delta\mathbf{r}) = N\exp\left\{-\frac{1}{2}\left[\boldsymbol{\sigma}\cdot\left(\bar{\mathbf{r}}-\mathbf{q}+\frac{\Delta\mathbf{r}}{2}\right)\right]^2\right\}$$

$$\times \exp\left\{-\frac{1}{2}\left[\sigma\cdot\left(\bar{\mathbf{r}}-\mathbf{q}-\frac{\Delta\mathbf{r}}{2}\right)\right]^2\right\}. \quad \text{(A6)}$$

In Eq. (A6) $N=\sigma_x\sigma_y\sigma_z/\pi^{3/2}$. One readily sees from the definition that the components of $\mathsf{T}(\mathbf{q})$ may be expressed

$$\mathsf{T}_{ab}(\mathbf{q}) = -\frac{1}{(2\pi)^3}\int\int\int \Upsilon(\bar{\mathbf{r}},\Delta\mathbf{r}) f(\sigma;\mathbf{q}|\bar{\mathbf{r}},\Delta\mathbf{r}) \times \nabla_a\nabla_b \exp(i\,\mathbf{k}\cdot\Delta\mathbf{r}) d(\Delta\mathbf{r})\, d\bar{\mathbf{r}}\, d\mathbf{k}, \quad \text{(A7)}$$

where the gradient operators in Eq. (A7) operate on the components of $\Delta\mathbf{r}$. Integration of Eq. (A7) by parts gives

$$\mathsf{T}_{ab}(\mathbf{q}) = -\frac{1}{(2\pi)^3}\int\int\int \exp(i\mathbf{k}\cdot\Delta\mathbf{r})\nabla_a\nabla_b \times [\Upsilon(\bar{\mathbf{r}},\Delta\mathbf{r}) f(\sigma;\mathbf{q}|\bar{\mathbf{r}},\Delta\mathbf{r})]\, d\Delta\mathbf{r}\, d(\bar{\mathbf{r}})\, d\mathbf{k}. \quad \text{(A8)}$$

Integration over $\mathbf{k}$ gives $(2\pi)^3\delta(\Delta\mathbf{r})$, so that Eq. (A8) becomes

$$\mathsf{T}_{ab}(\mathbf{q}) = -\int \tau_{ab}(\sigma;\mathbf{q}|\bar{\mathbf{r}})\, d\bar{\mathbf{r}}, \quad \text{(A9)}$$

where we have defined

$$\tau_{ab}(\sigma;\mathbf{q}|\bar{\mathbf{r}}) = \nabla_a\nabla_b[\Upsilon(\bar{\mathbf{r}},\Delta\mathbf{r}) f(\sigma;\mathbf{q}|\bar{\mathbf{r}},\Delta\mathbf{r})]_{\Delta\mathbf{r}=0}. \quad \text{(A10)}$$

Applying the chain rule to Eq. (A10) yields four terms, and from the definition of $f(\sigma;\mathbf{q}|\bar{\mathbf{r}},\Delta\mathbf{r})$ it can be shown that the cross terms are identically zero when $\Delta\mathbf{r}=0$. Thus after differentiation one obtains

$$\tau_{ab}(\sigma;\mathbf{q}|\bar{\mathbf{r}},) = f(\sigma;\mathbf{q}|\bar{\mathbf{r}},\Delta\mathbf{r})\nabla_a\nabla_b\gamma(\bar{\mathbf{r}},\Delta\mathbf{r})|_{\Delta\mathbf{r}=0} + \Upsilon(\bar{\mathbf{r}},\Delta\mathbf{r})\nabla_a\nabla_b f(\sigma;\mathbf{q}|\bar{\mathbf{r}},\Delta\mathbf{r})|_{\Delta\mathbf{r}=0}. \quad \text{(A11)}$$

Again from the definition of $f(\sigma;\mathbf{q}|\bar{\mathbf{r}},\Delta\mathbf{r})$ it can be shown that if $a\neq b$ then the second term in Eq. (A11) is identically zero. However if $a=b$ then the second term is in general nonzero and we have for $\tau_{ab}(\sigma;\mathbf{q}|\bar{\mathbf{r}})$:

$$\tau_{ab}(\sigma;\mathbf{q}|\bar{\mathbf{r}}) = \nabla_a\nabla_b\Upsilon(\bar{\mathbf{r}},\Delta\mathbf{r})|_{\Delta\mathbf{r}=0}\exp\{-[\sigma\cdot(\bar{\mathbf{r}}-\mathbf{q})]^2\} \quad a\neq b,$$

$$\tau_{aa}(\sigma;\mathbf{q}|\bar{\mathbf{r}}) = [\nabla_a^2\Upsilon(\bar{\mathbf{r}},\Delta\mathbf{r})|_{\Delta\mathbf{r}=0} - \sigma_a^2\rho(\bar{\mathbf{r}})]\exp\{-[\sigma\cdot(\bar{\mathbf{r}}-\mathbf{q})]^2\}, \quad \text{(A12)}$$

where $\rho(\bar{\mathbf{r}})=\gamma(\bar{\mathbf{r}}|\bar{\mathbf{r}})=\Upsilon(\bar{\mathbf{r}},0)$ is the one-electron position density. As prescribed by Eq. (A9) integration of $\tau_{ab}(\sigma;\mathbf{q}|\bar{\mathbf{r}})$ over the variables $\bar{\mathbf{r}}$ yields the components of the Husimi SMM tensor. To carry the analysis further requires detailed knowledge of the exact form of the density matrix. If the density matrix is expressed in a reasonable basis—as for example by a sum of Gaussian products—then the integrations are easily accomplished.

[1] M. A. Coplan, J. A. Tossell, and J. H. Moore, in *AIP Conference Proceedings No. 86, Momentum Wave Functions*, edited by E. Weigold (American Institute of Physics, New York, 1982), p. 82.
[2] A. Minchinton, Ref. 1, p. 115.
[3] J. P. D. Cook and C. E. Brion, Ref. 1, p. 278.
[4] A. Harmalker, A. M. Simas, V. H. Smith, Jr., and W. M. Westgate, Int. J. Quantum Chem. **23**, 811 (1983).
[5] P. Kaijer and V. H. Smith, Jr., Adv. Quantum Chem. **10**, 37 (1977).
[6] B. I. Ramirez, J. Phys. B **16**, 343 (1983).
[7] A. J. Thakkar, A. M. Simas, and V. H. Smith, Jr., J. Chem. Phys. **81**, 2953 (1984).
[8] A. M. Simas, V. H. Smith, Jr., and A. J. Thakkar, Int. J. Quantum Chem. Symp. **18**, 385 (1984).
[9] B. S. Sharma and A. J. Thakkar, Int. J. Quantum Chem. **24**, 323 (1986).
[10] A. J. Thakkar, B. S. Sharma, and T. Koga, J. Chem. Phys. **85**, 2845 (1986).
[11] R. G. Parr, K. Rupnik, and S. K. Ghosh, Phys. Rev. Lett. **56**, 1555 (1986).
[12] M. E. Casida, J. E. Harriman, and J. L. Anchell, Int. J. Quantum Chem. Symp. **21**, 435 (1987).
[13] J. L. Anchell and J. E. Harriman, J. Chem. Phys. **89**, 6860 (1988).
[14] A. C. Tanner, Chem. Phys. **123**, 241 (1988).
[15] C. A. Coulson, Proc. Cambridge Philos. Soc. **37**, 55 (1940).
[16] I. R. Epstein and A. C. Tanner, in *Compton Scattering*, edited by B. Williams (McGraw-Hill, New York, 1977).
[17] K. Husimi, Proc. Phys. Math Soc. Jpn. **22**, 264 (1940).
[18] J. E. Harriman, J. Chem. Phys. **88**, 6399 (1988).
[19] E. Wigner, Phys. Rev. **40**, 749 (1932).
[20] R. Krishnan, J. S. Binkley, R. Seeger, and J. A. Pople, J. Chem. Phys. **72**, 650 (1980).
[21] The original GAMESS (General Atomic and Molecular Electronic Structure System) program was assembled by the staff of the NRCC. M. Dupuis, D. Spangler, and J. J. Wendoloski, National Resource For Computations in Chemistry, Software Catalog, Vol. 1, Program QG01, 1980 Lawrence Berkeley Laboratory, USDOE.
[22] T. H. Dunning, Jr., J. Chem. Phys. **55**, 716 (1971).
[23] S. Huzinaga, J. Chem. Phys. **32**, 1595 (1960).
[24] W. J. Hehre, R. Ditchfield, and J. A. Pople, J. Chem. Phys. **56**, 2257 (1972).
[25] GAUSSIAN 86, M. J. Frisch, M. Head-Gordon, H. B. Schlegel, K. Raghavachari, J. S. Binkley, C. Gonzalez, D. J. Defrees, D. J. Fox, R. A. Whiteside, R. Seeger, C. F. Melius, J. Baker, L. R. Kahn, J. J. P. Stewart, S. Topiol, and J. A. Pople, Gaussian, Inc., Pittsburgh, PA (1988).
[26] J. E. Huheey, *Inorganic Chemistry*, 2nd ed. (Harper and Row, New York, 1978), Appendix F.
[27] D. F. Feller and K. Reudenberg, Theor. Chim. Acta (Berl.) **52**, 231 (1979).
[28] E. Wigner, Phys. Rev. **40**, 749 (1932).
[29] J. P. Dahl and M. Springborg, Mol. Phys. **47**, 1001 (1982).
[30] W. Yang, R. G. Parr, and C. Lee, Phys. Rev. A **34**, 4586 (1986).
[31] R. F. W. Bader and J. T. Preston, Int. J. Quantum Chem. **3**, 327 (1969).
[32] R. Baltin, J. Chem. Phys. **86**, 947 (1986).